Comparison of the speedy estimate methods of the induction motors

Thinh Cong Tran[1], Pavel Brandstetter[2], Hau Huu Vo[1], Chau Si Thien Dong[1], Martin Kuchar[2]
[1]Faculty of Electrical and Electronics Engineering, Ton Duc Thang University, Ho Chi Minh City, Vietnam
[2]Faculty of Electrical Engineering and Computer Science, VSB–Technical University of Ostrava, Ostrava City, Czech Republic

Article Info

Article history:

Received Aug 19, 2021
Revised Nov 15, 2022
Accepted Nov 25, 2022

Keywords:

Extended Kalman filter
Flux oriented control
GA algorithm
Induction motor drive
Sensorless
Speed estimation

ABSTRACT

This paper deals with a novel method to achieve the effective performance of the extended Kalman filter (EKF) for the speedy estimate of an induction motor. The real coding genetic algorithm (GA) is used to optimize the components of the covariance matrix in the EKF, thus ensuring the stability and accuracy of the filter in the speed estimation. The advantage of the proposed method is less dependent on the parameters of the induction motor. The content includes the vector control model for induction motor, the speed estimation by modeling the reference frame-model reference adaptive system (RF-MRAS), the current based-model reference adaptive system (CB-MRAS), and the speed estimation with the EKF optimized by genetic algorithm. Simulative studies on the field-oriented controller (FOC) with different operating conditions are performed in Matlab Simulink when the rotor resistance changes in the current speed estimation methods. The simulation results demonstrate the efficiency of the proposed GA-EKF filter compared with other speed estimation methods of induction motors.

Corresponding Author:

Thinh Cong Tran
Faculty of Electrical and Electronics Engineering, Ton Duc Thang University
19 Nguyen Huu Tho Street, Tan Phong Ward, District 7, Ho Chi Minh City, Vietnam
Email: trancongthinh@tdtu.edu.vn

1. INTRODUCTION

The control of the induction motor (IM) that has no speed sensor (sensorless) has the advantages such as low cost, high reliability, and saving space, reduces hardware, works well in chemical, dusty, decreases maintenance requirements. Due to the above advantages, there are now a number of methods for estimating the speed of induction motors without speed sensors studied such as the methods using the machine model is an estimative type of the open-loop [1], model reference adaptive system (MRAS) [2]-[7], the Luenberger observer [8]-[11], the sliding mode observer [12], the Kalman filter [13]-[18] (the first estimative types), and the methods which use machine models that are the estimator types using algorithms intelligent such as neural-networks [19]-[22], fuzzy-logic based on a control without the speedy sensor [23]-[25], (the second estimative types). Each method has its characteristics, advantages, and disadvantages, which will be presented below.

The MRAS is based on comparing the two outputs of the two models: the first model (the reference model) contains no the rotor speed, the second model (the adaptive model) uses the speed to estimate the flux of the induction motor. The outputs of the two models are compared together to get the error value. The error is the input of an appropriate adaptation mechanism to generate the estimated rate fed back to the adaptive model. The benefit of this method is simplicity, fast processing ability but low accuracy.

For the reasons mentioned above, this paper presents the method of the speed estimation by extended Kalman filter instead. It belongs to both groups mentioned above, because it uses the Kalman filter optimized by the genetic algorithm (GA), which has more advantages such as good noise filtering and higher accuracy. Since the equation of state of the induction motor is nonlinear, we will perform the discretization, and thus in each small cycle that is considered linear to apply the Kalman algorithm. This is a recursive problem combined with adaptation to estimate the parameters in the equation of the state of an induction motor. A notable problem in the Kalman filter is determining the components in the covariance matrix Q, R. Traditionally, we would define these matrices by trial and error method, but this method is time-consuming, and its accuracy is not high. Therefore, this paper presents how to determine these matrices by GA, which belongs to the second group, that of intelligent algorithms.

Except for the introduction and conclusion, this article includes four main sections. Section 1 is the modeling DFOC of the IM control without speed sensor, sections 2 is the speedy estimate method reference frame - model reference adaptive system (RF-MRAS), sections 3 is the speedy estimate method current based - model reference adaptive system (CB-MRAS), sections 4 includes details to implement the speedy estimate of the EKF: design of proposed EKF algorithm, determination of components of matrix Q, R by trial and error method, and GA algorithm. Finally, the simulation results of three methods in two cases: the resistance of rotor is constant and change during operation process.

The simulation results showed that the speed response of the Kalman filter optimized by GA is better than the RF-MRAS, CB-MRAS methods under different working conditions, when the rotor resistance varies with temperature. This also means that the GA-Kalman filter estimation method is less dependent on the system parameters than other methods. The studies covered in this introduction are presented in the next section.

2. THE MODELING DFOC OF INDUCTION MOTOR

From the equation system of an induction motor, the sensorless speed direct field-oriented control (SS-DFOC) for induction motor drive is constructed as following Figure 1 [26]-[29]. In this model, the proposed genetic algorithm - extended Kalman filter (GA-EKF) speedy estimate block with input parameters of voltage and current collected from the system through voltage and current sensors. The outputs are the estimated speed and flux current.

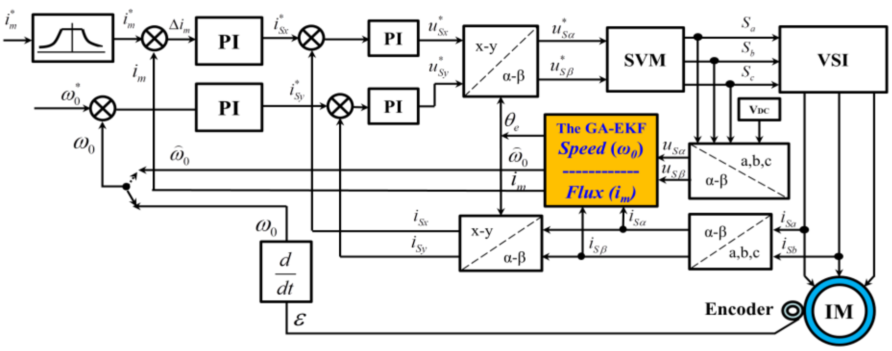

Figure 1. The structure of the SS-DFOC method

The vector control (FOC) includes controller of the stator currents characterized by a vector. This control is based on the design that converts a three-phase time and speed system into a two co-ordinate (x and y co-ordinate) time invariable system. This design lead to a configuration similar to a DC machine control. Vector controlled machines need two constants as input references: the torque cureent component represented by rotor speed ω_0 and the flux current component represented by I_m [26], [27].

3. ESTIMATE SPEED OF INDUCTION MOTOR USING MODEL RF-MRAS

3.1. The mathematical equations of the RF-MRAS model

The mathematical equations of the RF-MRAS model are as following [3]-[5].

$$\psi_{R\alpha} = \frac{L_r}{L_m}\left(\int\left(u_{s\alpha} - \hat{R}_s i_{s\alpha}\right)dt - \sigma L_s i_{s\alpha}\right) ; \psi_{R\beta} = \frac{L_r}{L_m}\left(\int\left(u_{s\beta} - \hat{R}_s i_{s\beta}\right)dt - \sigma L_s i_{s\beta}\right) \quad (1)$$

$$\hat{\psi}_{R\alpha} = \int\left(\frac{L_m}{T_r} i_{s\alpha} - \frac{1}{T_r}\hat{\psi}_{R\alpha} - \omega_0\hat{\psi}_{R\beta}\right) dt; \hat{\psi}_{R\beta} = \int\left(\frac{L_m}{T_r} i_{s\beta} - \frac{1}{T_r}\hat{\psi}_{R\beta} + \omega_0\hat{\psi}_{R\alpha}\right) dt \quad (2)$$

This model only cares about the motor speed, so the value of the stator resistor is known in the simulation. The error signal is represented below by the expression (with $K_P > 0, K_I > 0$).

$$\xi = \hat{\psi}_{R\alpha}\psi_{R\beta} - \hat{\psi}_{R\beta}\psi_{R\alpha};\ \hat{\omega}_0 = K_P\xi + K_I\int_0^t \xi dt \tag{3}$$

Where the state variables $i_{S\alpha}, i_{S\beta}, u_{S\alpha}, u_{S\beta}\psi_{R\alpha}, \psi_{R\beta}, \omega_0$ are stator currents, stator voltages, rotor fluxes, and the rotor speed of IM in $[\alpha - \beta]$ system, the parameters with a hat on the top are the estimated values.

3.2. The RF-MRAS model

The RF-MRAS for the speed estimation has diagram such as Figure 2 [6]. The model consists of two blocks: the adaptive block, and the reference block. Two these blocks are compared with each other, the difference in values of two these blocks is fed back to the adaptive block to correct the desired signal for accuracy. The current and voltage signals are specified in the model.

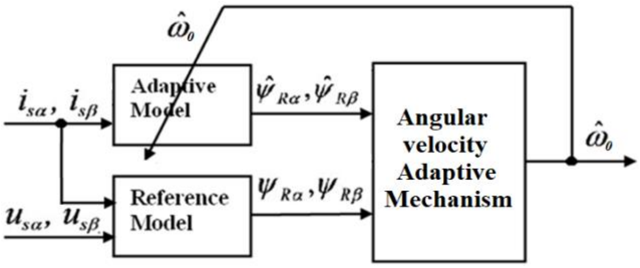

Figure 2. The diagram of speed estimation using the RF-MRAS model

4. ESTIMATE SPEED OF INDUCTION MOTOR USING MODEL CB-MRAS

4.1. The mathematical equations of the CB-MRAS model

The Mathematical equations of the CB-MRAS Model is described (4) [6], [7].

$$\hat{\imath}_{s\alpha} = \frac{1}{T_i}\int\left(K_1 u_{s\alpha} + K_2\hat{\psi}_{R\alpha} + K_3\hat{\omega}_R\hat{\psi}_{R\beta} - \hat{\imath}_{s\alpha}\right)dt;\ \hat{\imath}_{s\beta} = \frac{1}{T_i}\int\left(K_1 u_{s\beta} + K_2\hat{\psi}_{R\beta} - K_3\hat{\omega}_R\hat{\psi}_{R\alpha} - \hat{\imath}_{s\beta}\right)dt \tag{4}$$

The rotor speed is calculated from the following expression with $K_P > 0, K_I > 0$.

$$\xi = (i_{s\alpha} - \hat{\imath}_{s\alpha})\hat{\psi}_{R\beta} - \left(i_{s\beta} - \hat{\imath}_{s\beta}\right)\hat{\psi}_{R\alpha}, \hat{\omega}_r = K_P\xi + K_I\int_0^t \xi dt \tag{5}$$

$$\text{Where } K_1 = \frac{L_r}{C_1 L_m}; K_2 = \frac{L_m}{C_1(L_r\hat{R}_s T_r + L_m^2)}; K_3 = \frac{1}{C_1}; T_i = \frac{L_s L_r - L_m^2}{C_1 L_m}; C_1 = \frac{L_r\hat{R}_s}{L_m} + \frac{L_m}{T_r} \tag{6}$$

4.2. The CB-MRAS model

From the above expressions, the CB-MRAS model is built below [6]. Figure 3 is the CB-MRAS model which is similar to the RF-MRAS model, but the block functions differ from the above model. The model has three input blocks: current model, voltage model, and current estimation block. The output has two blocks: the rotor speed adaptive block, and the stator resistance adaptive block. Error signals: rotor speed and stator resistance are fed back to correct the rotor speed and stator resistance values.

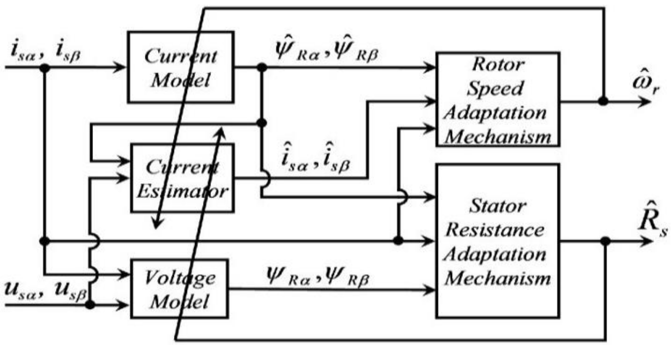

Figure 3. The diagram of speed estimation using CB-MRAS model

5. ESTIMATE THE SPEED OF IM USING EXTENDED KALMAN FILTER OPTIMIZED BY GA ALGORITHM

In this section, the first presents the discrete form model of the equations of state. The second is the algorithm to the EKF, how to determine the expressions in the algorithm, the Q matrix in the system block, R in the measurement block, and limitations in determining the matrix Q, R by trial and error. Finally, the GA algorithm (a smart algorithm) is used to optimally determine the components in the Q, R matrix for estimating the speed of the IM in the most accurate method.

5.1. Using EKF to estimate the speed of IM

From the nonlinear equations with five state variables: $i_{S\alpha}, i_{S\beta}, \psi_{R\alpha}, \psi_{R\beta}, \omega_0$ [26], [27], to be able to use the EKF recursively, They need to be transformed from the continuous state equations of the motor into a discrete form, and for each small cycle, these equations are considered linear. Then they are added into the system noise W and the measured noise V, so the EKF algorithm shown below [14]-[16] can be applied.

$$\begin{aligned} x_{n+1} &= A_n \cdot x_n + B_n \cdot u_n + W_n \\ y_{n+1} &= C_n \cdot x_{n+1} + V_n \end{aligned} \tag{7}$$

Here, the coefficient matrix is calculated according to the expression:

$$A_n = e^{AT} \approx I + AT; B_n = \int_0^T e^{AT} B dt \approx BT; C_n = C$$

$$x_{n+1} = \begin{bmatrix} i_{S\alpha}^{(n+1)} & i_{S\beta}^{(n+1)} & \lambda_{R\alpha}^{(n+1)} & \lambda_{R\beta}^{(n+1)} & \omega_0^{(n+1)} \end{bmatrix}^T; y_{n+1} = \begin{bmatrix} i_{S\alpha}^{(n+1)} & i_{S\beta}^{(n+1)} \end{bmatrix}^T; u_n = \begin{bmatrix} v_{S\alpha}^{(n)} & v_{S\beta}^{(n)} \end{bmatrix}^T$$

$$A_n = \begin{bmatrix} 1 - \frac{K_r}{K_l}T & 0 & \frac{L_h R_R}{L_R^2 K_l}T & \frac{P L_h \omega_0^n}{2 L_R K_l}T & 0 \\ 0 & 1 - \frac{K_r}{K_l}T & \frac{P L_h \omega_0^n}{2 L_R K_l}T & \frac{L_h R_R}{L_R^2 K_l}T & 0 \\ \frac{L_h}{T_r}T & 0 & 1 - \frac{1}{T_r}T & -\frac{P\omega_0^n}{2}T & 0 \\ 0 & \frac{L_h}{T_r}T & \frac{P\omega_0^n}{2}T & 1 - \frac{1}{T_r}T & 0 \\ -\frac{P L_h}{3 J L_R}\lambda_{R\beta}^n & \frac{P L_h}{3 J L_R}\lambda_{R\alpha}^n & 0 & 0 & 1 \end{bmatrix}; B_n = \begin{bmatrix} \frac{T}{K_l} & 0 \\ 0 & \frac{T}{K_l} \\ 0 & 0 \\ 0 & 0 \end{bmatrix}; C_n = \begin{bmatrix} 1 & 0 \\ 0 & 1 \\ 0 & 0 \\ 0 & 0 \\ 0 & 0 \end{bmatrix}^T \tag{8}$$

The covariance matrices Q and R of noises have the following form:

$$Q_n = Cov(w) = E[ww^t] = \begin{cases} Q_n \ with\ n = l \\ 0\ otherwise \end{cases}; R_n = Cov(v) = E[vv^t] = \begin{cases} R_n \ with\ n = l \\ 0\ otherwise \end{cases}$$

The matrices Q, R show that they have the form of diagonal matrices. The EKF algorithm is used for the speedy estimation model of the induction motors.

$$\overline{x}_{n+1} = A\hat{x}_n + Bu_n = f(x_i^n, u^n) \tag{9}$$

The linearization of nonlinear equation [26], [27] inplemented around the estimated value $\hat{x}_i$ is as following

$$F_n = \frac{\partial f_n(x_i^n, u^n)}{\partial x_i} = \frac{\partial (A\hat{x}_{n-1} + Bu_{n-1})}{\partial x_i} \tag{10}$$

$$\overline{P}_{n+1} = F_n \hat{P}_n F_n^T + Q \tag{11}$$

$$h(x_i^n) = C_n(x_i^n)x_i^n \tag{12}$$

$$H_n = \frac{\partial h(x_i^n)}{\partial x_i} = \frac{\partial (C_n(x_i^n)x_i^n)}{\partial x_i} \tag{13}$$

$$K_{n+1} = \overline{P_{n+1}} H^T (H\overline{P_{n+1}}H^T + R)^{-1} \tag{14}$$

$$\hat{x}_{n+1} = \overline{x}_{n+1} + K_{n+1}(y_{n+1} - C_n \overline{x}_{n+1}) \tag{15}$$

$$\widehat{P_{n+1}} = \overline{P_{n+1}} - K_{n+1} C \overline{P_{n+1}} \tag{16}$$

Where the P is covariance matrix. The K is the Kalman filter gain. The x are state variables (parameters) of IM. The noise matrix Q, R, and the parameters with a hat are the estimated values. The beginning value of the covariance error matrix has the form below.

$$Q = \begin{bmatrix} \lambda_1 & 0 & 0 & 0 & 0 \\ 0 & \lambda_2 & 0 & 0 & 0 \\ 0 & 0 & \lambda_3 & 0 & 0 \\ 0 & 0 & 0 & \lambda_4 & 0 \\ 0 & 0 & 0 & 0 & \lambda_5 \end{bmatrix}; R = \begin{bmatrix} \mu_1 & 0 \\ 0 & \mu_2 \end{bmatrix}; P = \begin{bmatrix} 1 & 0 & 0 & 0 & 0 \\ 0 & 1 & 0 & 0 & 0 \\ 0 & 0 & 1 & 0 & 0 \\ 0 & 0 & 0 & 1 & 0 \\ 0 & 0 & 0 & 0 & 1 \end{bmatrix}$$

To implement the EKF for estimating the rotor speed, current, and flux, the parameters λ_i, μ_i are appropriately chosen in the Q, R matrix. Traditionally, this is done by trial and error, which takes a long time but doesn't produce very good results. For this reason, we will find the optimal solution for determining the parameters of the fit of Q and R by genetic algorithm. The algorithm will be presented in the following section.

5.2. Using genetic algorithm to estimate parameters of Q, R of EKF

To find the optimal parameters λ_i, μ_i, we use a soft computational algorithm that is the GA [23], [30]. When the appropriate parameters are available, the motor speed estimation will be more accurate. The algorithm flowchart for finding parameters λ_i, μ_i of the matrix Q, R is below.

Figure 4 is the GA algorithm applied to this paper. In the first step of the algorithm, we randomly initialize the population (parameters Q, R) and encode the computation in the form of real numbers. This set of parameters will be transferred to the Matlab model to perform the simulation. Its results will be evaluated by the cost function, then perform genetic operations such as selection, crossover, and mutation. Thus, we will have a new set of values (usually better than the previous one) and continue to feed the model for testing. This process continues until the required number of generations reached. The result of the last run time is the best.

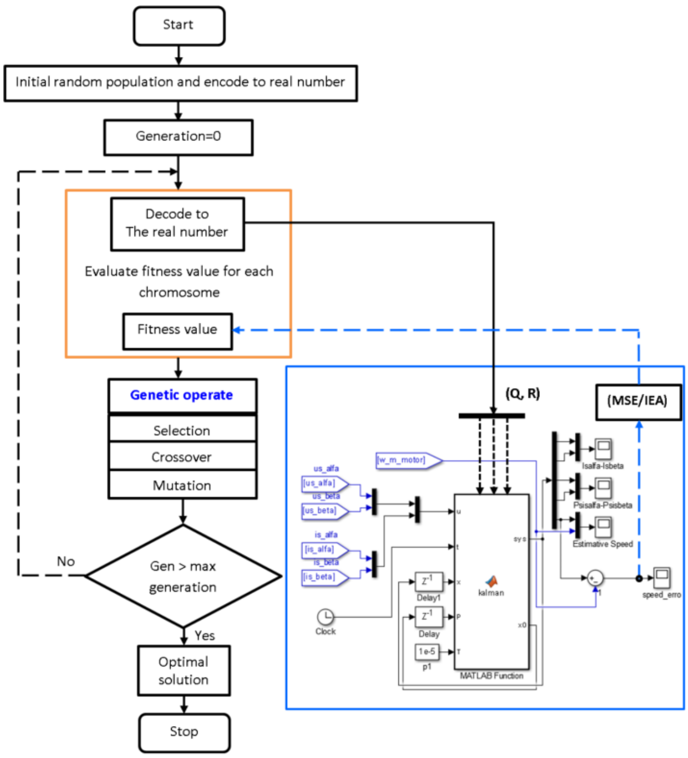

Figure 4. A flowchart of the genetic algorithm for the GA-EKF model

6. SIMULATION RESULTS AND ANALYSIS

The basic simulative parameters used for induction motors are as: P = 1.5 kW, U_{DC} = 270 V, P_P = 2, R_S = 2.1 Ω, R_r = 2.51 Ω, L_m = 0.129 H, L_S = 0.137 H, L_r = 0.137 H, J = 0.043 kg.m^2. The three different speed levels simulated in this section are 100 rpm, 40 rpm, and −40 rpm. The simulation results in many cases are presented in the following sections.

6.1. Estimate speed of IM based on the model, RF-MRAS

In the Figure 5 (the first figure of the simulation), the responses of the reference speed and the actual speed are shown. The solid line is the reference speed. The dashed line is the response of the actual speed. The actual speed follows the desired speed, but there is an overshoot. Figure 6 the comparison of Figure 6(a) the RF-MRAS estimated speed, the actual speed, and the reference speed and the relationship of Figure 6(b) the error between the estimated speed and the actual speed, we see that the speed error between the RF-MRAS estimated speed and the actual speed is large. Its peak value is 13 rpm, so this method is used in drives less than at present.

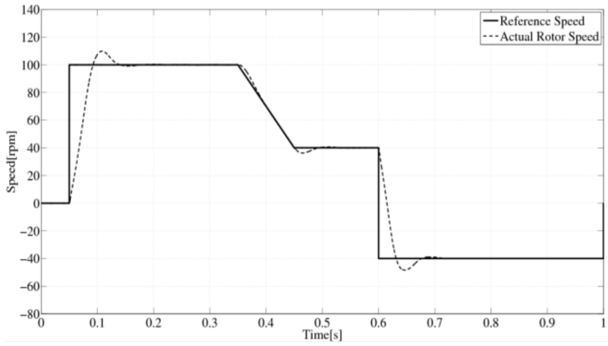

Figure 5. Reference and actual rotor speed of the IM drive

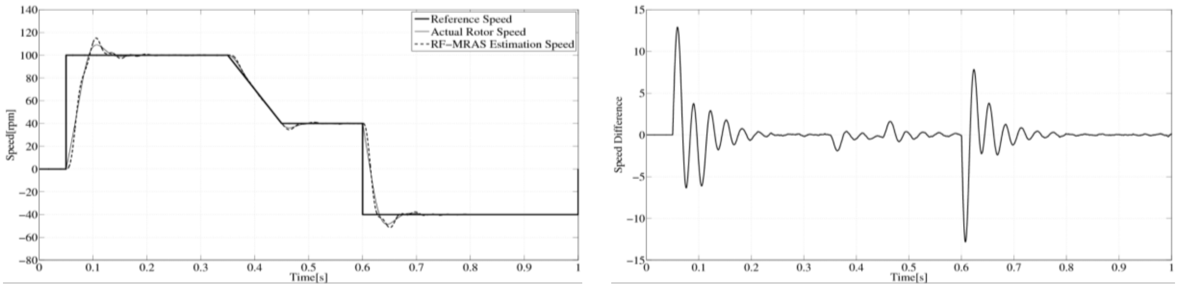

(a) (b)

Figure 6. The comparison of (a) the RF-MRAS estimated speed and (b) the error between RF-MRAS estimated speed and actual speed

6.2. Estimate speed of IM based on CB-MRAS model

This section is the simulated results of the CB-RAS model. Figure 7 the evaluation of Figure 7(a) the CB-RAS estimated speed, the reference speed, and the actual speed and the analysis of Figure 7(b) the speedy error between the CB-RAS estimated model and the actual model, the deviation of the estimated speed of the CB-MRAS model is quite good. Its peak value is 2.7 rpm.

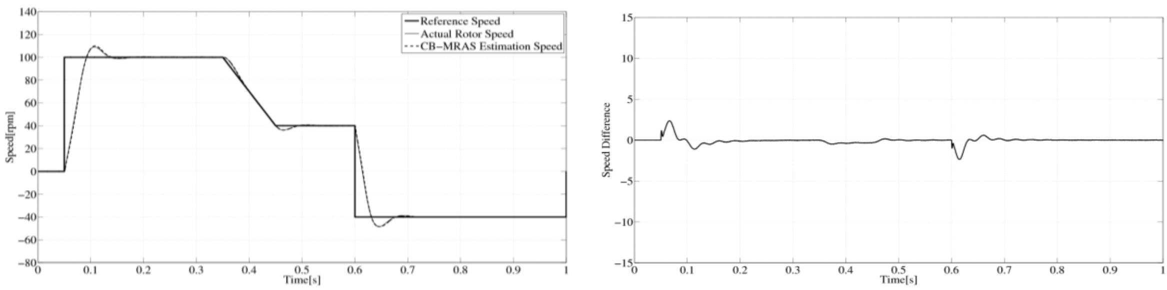

(a) (b)

Figure 7. The evaluation of (a) the CB-MRAS estimated speed and (b) the error between the CB-MRAS estimated speed and the actual speed

6.3. Estimate speed of IM based on EKF with defining matrices Q, R by trial and error

First, the values λ_i, μ_i in the matrix Q, R which is chosen by trial and error are: λ_1 = 9.23E-14; λ_2 = 8.33E-14; λ_3 = 4.88E-14; λ_4 = 6.85E-08; λ_5 = 1.46E-08; μ_1 = 9.13E-05; μ_2 = 4.99E-06. With these values, the speedy response is shown in the Figure 8. The speed according to EKF algorithm is the dashed line. These values cause a divergence with a spiked error. This method takes a lot of time, but the results obtained are not optimal. We continue to probe by trial and error. The selected values are: λ_1 = 8.74E-14; λ_2 = 4.26E-14; λ_3 = 1.69E-14; λ_4 = 6.80E-14; λ_5 = 3.26E-08; μ_1 = 1.79E-05; μ_2 = 2.49E-05. With the new values for EKF method by trial and error, the speed response is displayed in the Figure 9. Its error is a small value that we can see in this figure with the dashed line.

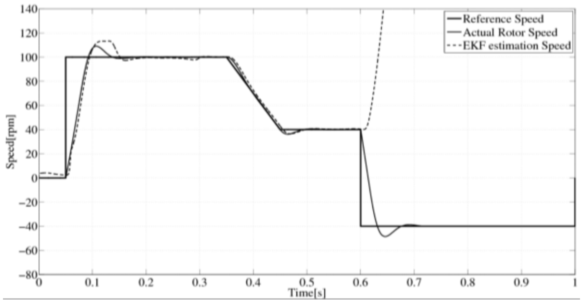

Figure 8. The reference, actual rotor, and EKF estimated speed

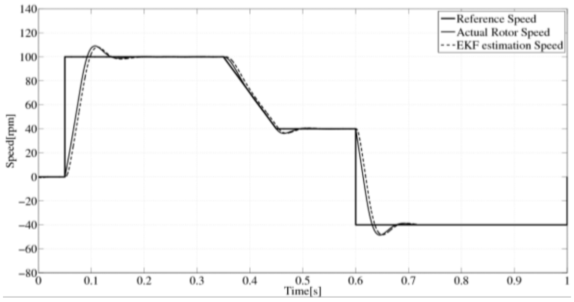

Figure 9. Reference, actual rotor, and new EKF estimated speed

6.4. Estimate speed of IM based on EKF with defining matrices Q, R by GA algorithm

The two matrices Q and R are diagonal matrices of seven values that need to be determined. If the values (λ_1, λ_2, λ_3, λ_4, λ_5, μ_1, μ_2) are chosen by trial and error, it takes a long time, but the results described above are not very good. Because of this reason, the components in the matrix are found by the genetic algorithm to save time and get the best speedy estimation response. The Table 1 includes parameters of GA algorithm that we will use to find optimal values for two matrices Q and R. The range of values for variables is [1e-18-0.1]. The cost function is calculated according to the error MSE is $E = \frac{1}{n}\sum_1^n (S_{real\_speed} - S_{estimated\_speed})^2$.

After performing the GA algorithm according to the diagram of Figure 4, we below collect results in the Table 2. Ten rows of the table correspond to 10 implementations of the GA algorithm. Columns $\lambda_1, \lambda_2, \lambda_3, \lambda_4, \lambda_5$ are of the Q matrix and columns μ_1, μ_2 are of the R matrix. The MSE column is the speed error corresponding to 10 runs of the algorithm.

The best values after ten runs substituted into the matrix Q, R have the results shown below. Figure 10 the analysis of Figure 10(a) the actual rotor speed, the GA_EKF speed, and the reference speed and the comparison of Figure 10(b) speed error between the GA_EKF model and the actual model. This speed error is the smallest compared to the two methods investigated above, the RF-MRAS and the CB-MRAS. Its peak value is less than 2 rpm, so this method can be used for IM drives.

Table 3 is the results of the speedy error comparison. They consist of the RF-MRAS, the CB-MRAS, and the GA-EKF methods by the least squares method. The RF-MRAS Method has an error of 4.5502 rpm, the CB-MRAS method has an error of 0.1896 rpm, and the GA-EKF Method has an error of 0.0839.

Table 1. The parameters of GA algorithm

Parameters	Values
Population size	60
The crossover probability	0.5
The mutative probability	0.02
Number of generations	10

Simulation results of three methods, including graphs and errors evaluated according to MSE-standard, are presented above. In the proposed new method, the extended Kalman filter in which the parameters are optimized by the GA algorithm shows its advantages. These can conclude that the GA-EKF method is the best, although the CB-MRAS method was considered the best for a long time before.

Table 2. Convergence results after ten repetitions

Index	λ_1	λ_2	λ_3	λ_4	λ_5	μ_1	μ_2	MSE
1	4.82E-03	2.90E-10	2.90E-10	2.52E-09	5.84E-17	9.83E-03	5.84E-05	7.1586
2	7.30E-15	1.08E-18	5.83E-08	5.84E-17	7.30E-15	0.042825	9.83E-14	5.0869
3	2.98E-21	2.90E-10	4.28E-02	8.65E-01	4.87E-09	1.01E-04	9.65E-04	3.2586
4	4.61E-02	7.82E-01	9.89E-01	5.31E-01	7.50E-01	1.12E-05	9.83E-04	2.1869
5	4.84E-08	7.82E-07	9.89E-09	5.31E-07	7.50E-11	1.12E-04	2.92E-05	1.0821
6	4.84E-08	7.82E-07	9.89E-09	5.31E-07	7.50E-11	1.12E-04	2.92E-05	1.0821
7	6.97E-11	2.90E-10	9.89E-05	8.65E-01	9.90E-01	1.01E-07	2.28E-06	0.5735
8	2.26E-10	3.44E-12	2.26E-06	1.21E-12	9.83E-14	6.17E-06	6.17E-07	0.1286
9	7.30E-15	3.85E-07	7.30E-15	7.61E-18	4.82E-10	3.85E-07	2.26E-06	0.0870
10	2.65E-12	3.44E-16	2.65E-12	8.18E-18	2.26E-12	1.21E-07	1.21E-07	0.0839

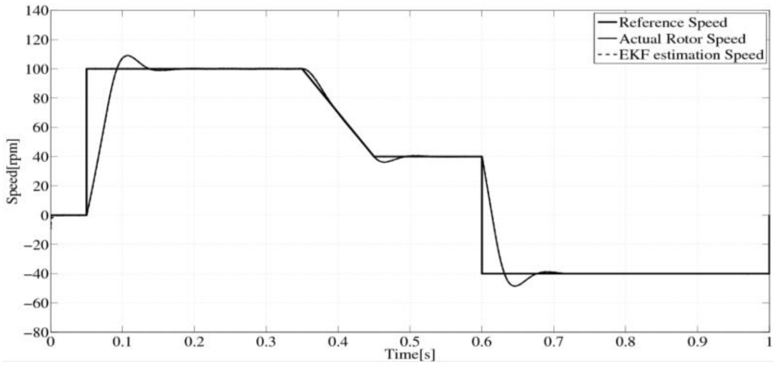

(a)

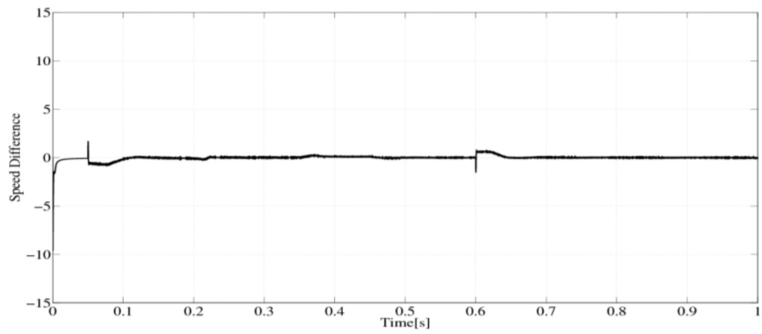

(b)

Figure 10. The analysis of (a) the EKF estimated speed and (b) the error between real speed and the EKF estimated speed

Table 3. The error of the three methods

The methods	$E = \frac{1}{n}\sum_{1}^{n}(S_{real\_speed} - S_{estimated\_speed})^2$	The evaluated results
RF-MRAS	4.5502	Good
CB-MRAS	0.1896	Very good
GA-EKF	0.0839	The best

6.5. The responses of the estimated speed in the cases of variable rotor resistance

6.5.1. The resistance (R_r) changes from 2.51 Ω to 2.0 Ω

During operation, the resistance of the rotor (R_r) can be changed by temperature, this also means that the rotor time constant (T_r) changes, it is a significant parameter in induction motors which affect the process of motor speed estimation. Therefore, its influence is considered in the three-speedy estimation methods mentioned above. In this section, the variable rotor resistance value and its influence on the speed estimation methods are investigated. The results of the three models are displayed in Figure 11. The variation of Figure 11(a) the rotor resistance value from 2.51 Ω to 2.0 Ω and the comparison of Figure 11(b) the estimated speed of the RF-MRAS model, Figure 11(c) the estimated speed of the CB-MRAS model, and Figure 11(d) the estimated speed of the GA-EKF model, this is one of the cases in which the rotor resistance can change during operation.

The simulated characteristics and results of all three methods which are mentioned above are summarized in Table 4. The first column of this table is the methods. The second column is the speed error. Finally, the third column is the evaluation result for each method.

The results are obtained from the graphs and the calculation of the error according to the MSE standard, when the rotor resistance reduced by 20%. In third column, we see that the error of the GA-EKF method is the smallest (11.1203 rpm) and the speedy error of the RF-MRAS method is the largest. These show that the CB-MRAS method is better than RF-MRAS, but the EKF method is the best.

Table 4. The error of the three methods (the Rr changes from 2.51Ω to 2.0Ω)

The methods	$E = \frac{1}{n}\sum_{1}^{n}(S_{real\_speed} - S_{estimated\_speed})^2$	The evaluated results
RF-MRAS	22.0262	Quite good
CB-MRAS	12.4048	Good
GA-EKF	11.1203	Good

6.5.2. The resistance (R_r) changes from 2.51 Ω to 3.0 Ω

Other changes in the rotor resistance are studied continually in this section. Now we will examine the case of increased resistance. From the simulation results, we obtain the graphs as well as the calculation of the speedy errors that will be presented in the following section. This section is similar to the one above. The results of all models are shown below. Figure 12 the change, Figure 12(a) of the rotor resistance value from 2.51 Ω to 3.0 Ω and the relationship of Figure 12(b) the estimated speed of the RF-MRAS model, Figure 12(c) the estimated speed of the CB-MRAS model, and Figure 12(d) the estimated speed of the GA-EKF model, this part compares the estimated speedy responses of all models in the change of the rotor resistance.

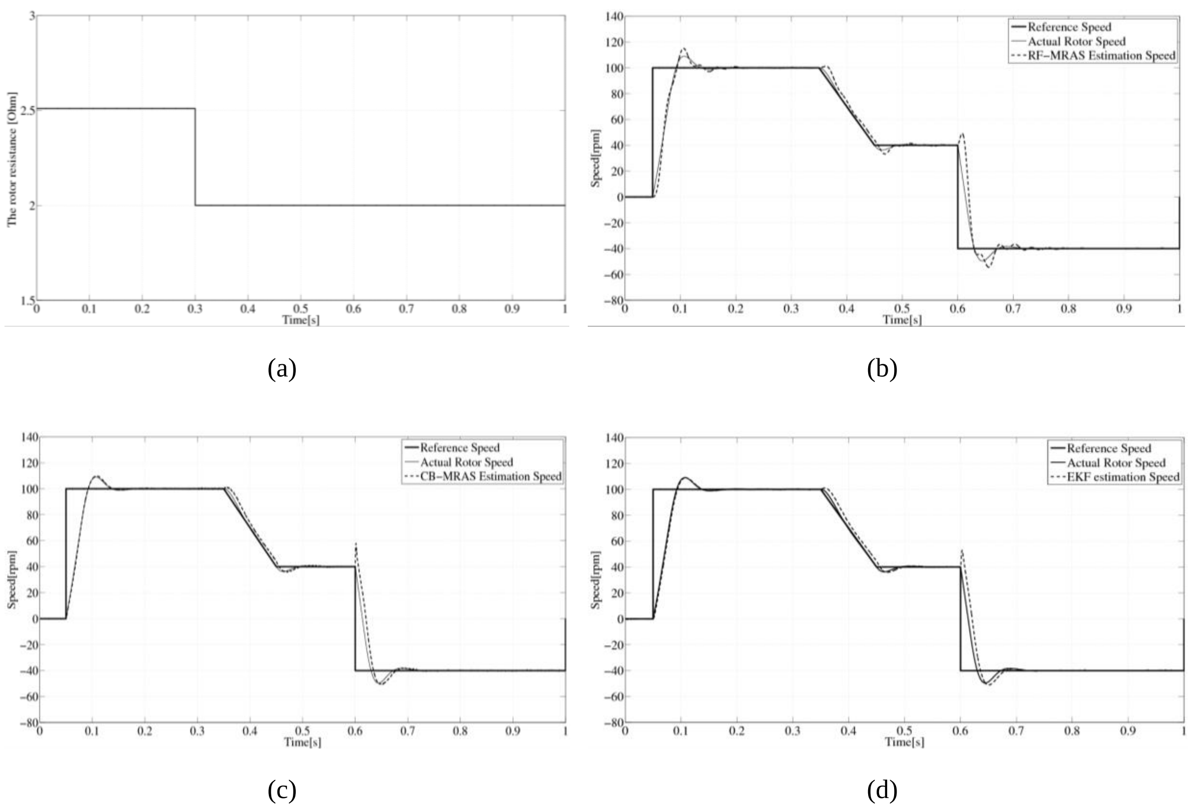

Figure 11. The variation of (a) the change value of the rotor resistance, (b) the RF-MRAS model, (c) the CB-MRAS model, and (d) the GA-EKF model

All simulation results are listed in Table 5. Similar to Table 4, this Table 5 also summarizes the estimated results of all three methods: the RF-MRAS, the CB-MRAS, and the GA-EKF in the case of increased rotor resistance. The first column of this Table 5 the methods. The second column is the speed error. Finally, the third column is the evaluation results of each method.

In this case, the rotor resistance increased to 20%. We evaluate the speed error according to the MSE standard. The RF-MRAS method has the largest error (13.5012 rpm), while the other two methods are quite good and approximately equal. These obtained results show that the GA-EKF method is equivalent to the CB-MRAS, and both these methods are better than the RF-MRAS method.

Table 5. The error of the three methods (the R_r changes from 2.51 Ω to 3.0 Ω)

The methods	$E = \frac{1}{n}\sum_{1}^{n}(S_{real\_speed} - S_{estimated\_speed})^2$	The evaluated results
RF-MRAS	13.5012	Quite good
CB-MRAS	7.1828	Good
GA-EKF	7.2734	Good

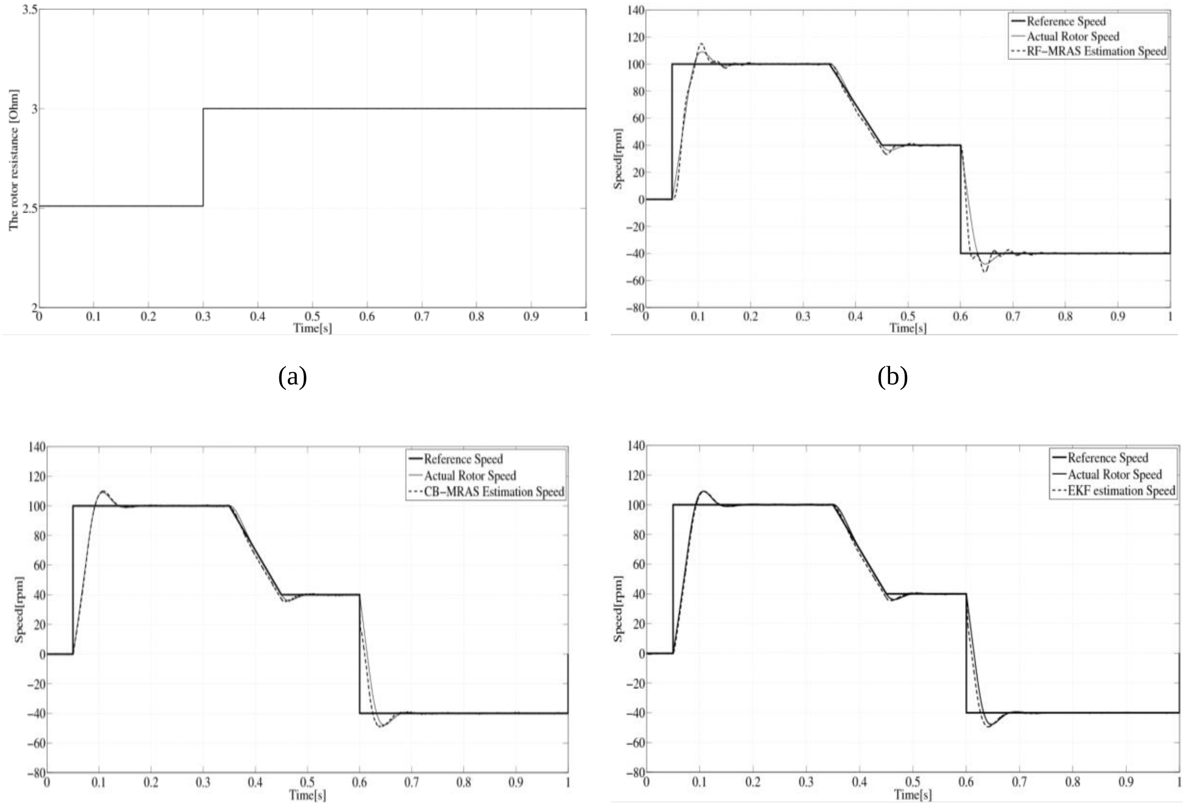

Figure 12. The change (a) Rotor resistance, (b) The RF-MRAS, (c) The CB-MRAS, and (d) The EKF estimated speed

7. CONCLUSION

This paper presents three methods of speed estimation of IM: the RF-MRAS, the CB-MRAS, and the GA-EKF. Particularly, it focuses on the speedy estimation method using the GA-EKF algorithm with the system noise matrix Q and the measured noise matrix R optimized by the GA algorithm. Simulation results in cases of variable rotor resistance (constant, decrease, or increase). In the case of constant rotor resistance, the CB-MRAS method is much better than RF-MRAS, but the GA-EKF method is also much better than the CB-MRAS. In the case of reduced rotor resistance, the CB-MRAS speed estimation method is also much better than RF-MRAS, but the GA-EKF method is better than CB-MRAS. With the increased rotor resistance, the CB_MRAS method is much better than the RF-MRAS, and the GA-EKF method approximates the CB-MRAS. Thus, in most cases: variable or unchanged rotor resistance, the GA-EKF speed estimation method optimized by the GA algorithm which is presented in this paper can claim to be the best, although the CB-MRAS speedy estimation method was considered the best in a long time before.

It can see that the proposed GA-EKF model is less dependent on the induction motor parameters than the RF-MRAS and the CB-MRAS model, but the GA-EKF model is the most complex of the mentioned models. Therefore, a DSP processor must be used when implementing the GA-EKF algorithm. Today with the strong development of semiconductor technology, this method is easily implemented in industrial devices.

REFERENCES

[1] T. C. Tran, P. Brandstetter, and H. H. Vo, "The Sensorless Speed Controller of Induction Motor in DFOC Model Based on the Voltage and Current," *Journal of Advanced Engineering and Computation (JAEC)*, vol. 3, no. 1, 2019, doi: 10.25073/jaec.201931.228.

[2] V. Verma and C. Chakraborty, "New series of MRAS for speed estimation of vector controlled induction motor drive," *IECON 2014 - 40th Annual Conference of the IEEE Industrial Electronics Society*, 2014, pp. 755-761, doi: 10.1109/iecon.2014.7048585.

[3] A. Kadrine, Z. Tir, O. P. Malik, M. A. Hamida, A. Reatti, and A. Houari, "Adaptive non-linear high gain observer based sensorless speed estimation of an induction motor," *Journal of the Franklin Institute*, vol. 357, no. 13, pp. 8995-9024, 2020, doi: 10.1016/j.jfranklin.2020.06.013.

[4] W. El Merrassi, A. Abounada, and M. Ramzi, "Advanced speed sensorless control strategy for induction machine based on neuro-MRAS observer," *Materials Today: Proceedings*, 2021, vol. 45, no. 8, pp. 7615-7621, doi: 10.1016/j.matpr.2021.03.081.

[5] Z. Yang, Q. Ding, X. Sun, C. Lu, and H. Zhu, "Speed sensorless control of a bearingless induction motor based on sliding mode observer and phase-locked loop," *ISA Transactions*, vol. 123, pp. 346-356, 2022, doi: 10.1016/j.isatra.2021.05.041.

[6] T. O. -Kowalska and M. Dybkowski, "Stator-Current-Based MRAS Estimator for a Wide Range Speed-Sensorless Induction-Motor Drive," *IEEE Transactions on Industrial Electronics*, vol. 57, no. 4, pp. 1296-1308, 2010, doi: 10.1109/TIE.2009.2031134.

[7] A. Bosso, A. Tilli, and C. Conficoni, "A Robust Sensorless Controller-Observer Strategy for PMSMs with Unknown Resistance and Mechanical Model," *IFAC-PapersOnLine*, vol. 53, no. 2, pp. 1536-1542, 2020, doi: 10.1016/j.ifacol.2020.12.2014.

[8] A. Bıçak and A. Gelen, "Sensorless direct torque control based on seven-level torque hysteresis controller for five-phase IPMSM using a sliding-mode observer," *Engineering Science and Technology, an International Journal*, vol. 24, no. 5, pp. 1134-1143, 2021, doi: 10.1016/j.jestch.2021.02.004.

[9] M. L. Jayaramu, H. N. Suresh, M. S. Bhaskar, D. Almakhles, S. Padmanaban, and U. Subramaniam, "Real-time implementation of extended kalman filter observer with improved speed estimation for sensorless control," *IEEE Access*, vol. 9, pp. 50452-50465, 2021, doi: 10.1109/ACCESS.2021.3069676.

[10] L. Zhang, Z. Dong, L. Zhao, and S. Laghrouche, "Sliding mode observer for speed sensorless linear induction motor drives," *IEEE Access*, vol. 9, pp. 51202-51213, 2021, doi: 10.1109/ACCESS.2021.3067805.

[11] J. Gacho and M. Žalman, "IM Based Speed Servodrive with Luenberger Observer", *Journal of Electrical Engineering*, vol. 61, no. 3, pp. 149-156, 2010, doi: 10.2478/v10187-011-0021-8.

[12] O. Çetin, A. Dalcalı, and F. Temurtaş, "A comparative study on parameters estimation of squirrel cage induction motors using neural networks with unmemorized training," *Engineering Science and Technology, an International Journal*, vol. 23, no. 5, pp. 1126-1133, 2020, doi: 10.1016/j.jestch.2020.03.011.

[13] P. Brandstetter and M. Dobrovsky, "Speed Estimation of Induction Motor Using Model Reference Adaptive System with Kalman Filter," *Advances in Electrical and Electronic Engineering*, vol. 12, no. 1, pp. 22-28, 2013, doi: 10.15598/aeee.v11i1.802.

[14] A. Namdar, H. Samet, M. Allahbakhshi, M. Tajdinian, and T. Ghanbari, "A robust stator inter-turn fault detection in induction motor utilizing Kalman filter-based algorithm," *Measurement*, vol. 187, 2022, doi: 10.1016/j.measurement.2021.110181.

[15] R. Yildiz, M. Barut, and E. Zerdali, "A comprehensive comparison of extended and unscented Kalman filters for speed-sensorless control applications of induction motors," *IEEE Transactions on Industrial Informatics*, vol. 16, no. 10, pp. 6423-6432, 2020, doi: 10.1109/tii.2020.2964876.

[16] L. Et-Taaj, Z. Boulghasoul, A. Elbacha, and A. El Kharki, "Robust sensorless Induction Motor control based on Extended Kalman Filter observer," in *2021 International Congress of Advanced Technology and Engineering (ICOTEN)*, 2021, pp. 1-9, doi: 10.1109/ICOTEN52080.2021.9493502.

[17] J. Kim, Y. Lee, and J. Lee, "A sensorless speed estimation for indirect vector control of three-phase induction motor using Extended Kalman Filter," in *2016 IEEE Region 10 Conference (TENCON)*, 2016, pp. 3087-3090, doi: 10.1109/tencon.2016.7848616.

[18] Y. Laamari, K. Chafaa, and B. Athamena, "Particle Swarm Optimization of An Extended Kalman Filter for Speed and Rotor Flux Estimation of an Induction Motor," *Electrical Engineering*, vol. 97, pp. 129-138, 2015, doi: 10.1007/s00202-014-0322-1.

[19] J. -C. G. -Real, V. M. -Martínez, and J. G. -Gil, "ANN-based position and speed sensorless estimation for BLDC motors," *Measurement*, vol 188, 2022, doi: 10.1016/j.measurement.2021.110602.

[20] Z. Yang, D. Wang, X. Sun, and J. Wu, "Speed sensorless control of a bearingless induction motor with combined neural network and fractional sliding mode," *Mechatronics*, vol. 82, 2022, doi: 10.1016/j.mechatronics.2021.102721.

[21] K. Xu and S. Liu, "Speed-sensorless vector control based on ANN MRAS for induction motor drives," *Journal of Advanced Computational Intelligence and Intelligent Informatics*, vol. 19, no. 1, pp. 127-133, 2015, doi: 10.20965/jaciii.2015.p0127.

[22] S. M. Gadoue, D. Giaouris, and J. W. Finch, "Sensorless Control of Induction Motor Drives at Very Low and Zero Speeds Using Neural Network Flux Observer," *IEEE Transactions on Industrial Electronics*, vol. 56, no. 8, pp. 3029–3039, 2009, doi: 10.1109/TIE.2009.2024665.

[23] T. C. Tran, P. Brandstetter, C. D. Tran, S. D. Ho, M. C. H. Nguyen, and P. N. Phuong, "Parameters estimation for sensorless control of induction motor drive using modify GA and CSA algorithm," in *International Conference on Advanced Engineering Theory and Applications*, 2018, pp. 580-591, doi: 10.1007/978-3-030-14907-9_57.

[24] R. N. Mishra and K. B. Mohanty, "Development and implementation of induction motor drive using sliding-mode based simplified neuro-fuzzy control," *Engineering Applications of Artificial Intelligence*, vol. 91, 2020, doi: 10.1016/j.engappai.2020.103593.

[25] M. Nikpayam, M. Ghanbari, A. Esmaelia, and M. Jannati, "Fault-tolerant control of Y-connected three-phase induction motor drives without speed measurement," *Measurement*, vol. 149, 2020, doi: 10.1016/j.measurement.2019.106993.

[26] P. Vas, *Sensorless Vector and Direct Torque Control*, LDN, UK: Oxford University Press, 1998. [Online]. Available: http://books.google.com/books?id=9ORSAAAAMAAJ

[27] S. El Daoudi, L. Lazrak, N. El Ouanjli, and M. A. Lafkih, "Sensorless fuzzy direct torque control of induction motor with sliding mode speed controller," *Computers and Electrical Engineering*, vol. 96, 2021, doi: 10.1016/j.compeleceng.2021.107490.

[28] P. Brandstetter, M. Dobrovsky, and M. Kuchar, "Implementation of genetic algorithm in control structure of induction motor AC drive," *Advances in Electrical and Computer Engineering*, vol. 14, no. 4, pp. 15-20, 2014, doi: 10.4316/aece.2014.04003.

[29] C. D. Tran, P. Palacky, M. Kuchar, P. Brandstetter, and B. H. Dinh, "Current and speed sensor fault diagnosis method applied to induction motor drive," *IEEE Access*, vol. 9, pp. 38660-38672, 2021, doi: 10.1109/access.2021.3064016.
[30] A. C. Megherbi, H. Megherbi, K. Benmahamed, A. G. Aissaoui, and A. Tahour, "Parameter identification of induction motors using variable-weighted cost function of genetic algorithms," *Journal of electrical engineering and technology*, vol. 5, no. 4, pp. 597-605, 2010, doi: 10.5370/JEET.2010.5.4.597.

BIOGRAPHIES OF AUTHORS

Thinh Cong Tran was born in Da Nang City, Vietnam. He received his M.Sc. degree in Electrical and Electronic Engineering from National University of Technology, Ho Chi Minh City, Vietnam in 1998. He received his PhD degree in Electrical Engineering and Computer Science from VSB - Technical University of Ostrava, Czech Republic in 2018. Now, he is teaching at department of electrical and electronics engineering (FEEE), Ton Duc Thang University, Ho Chi Minh city, Vietnam. His research interests include microcontroller systems, power electronic, modern control methods of electrical drives, soft computing algorithms, and optics. He can be contacted at email: trancongthinh@tdtu.edu.vn.

Pavel Brandstetter was born in Ostrava, Czech Republic, 1955, 1 June. He received the M.Sc. and Ph.D. degrees in Electrical Engineering from Brno University of Technology, Czech Republic, in 1979 and 1987, respectively. He is currently a full professor in Electrical Machines, Apparatus and Drives and dean of Faculty of Electrical Engineering and Computer Science at VSBTechnical University of Ostrava. Research activities include modern control methods of AC drives, for example, sensorless control of the IM and PMSM drives using different types of the observers. He can be contacted at email: pavel.brandstetter@vsb.cz.

Hau Huu Vo finished his Ph.D. at Ostrava Technical University (VSB-TUO), the Czech Republic in 2017. He is a Lecturer at the Faculty of Electrical and Electronic Engineering (FEEE), Ton Duc Thang University (TDTU), Vietnam. He published 5 journal articles and 10 conference papers. He is interested in intelligent electric motors, control, and robotics. He can be contacted at email: vohuuhau@tdtu.edu.vn.

Chau Si Thien Dong obtained her PhD degree from VSB-TUO, Czech Republic in 2017. She is now dean of FEEE, TDTU, Vietnam. She has published 15 conference papers and 5 journal papers. Her research interests focus on modern control and drives. She can be contacted at email: dongsithienchau@tdtu.edu.vn.

Martin Kuchar was born in Ostrava, Czech Republic, in 1977. He received the M.Sc. and Ph.D. degrees in Electrical Engineering from VSB-Technical University of Ostrava, Czech Republic, in 2000 and 2003, respectively. He worked as an R&D Engineer in practice for almost 10 years. Now he is an Associate Professor in Electrical Engineering in the Department of Electronics, Faculty of Electrical Engineering and Computer Science, VSBTechnical University of Ostrava. His research interests include DSC based control systems, sensorless and sensor fault tolerant control of AC drives, applications of observers, estimators and soft computing methods in the control of electrical drives. He can be contacted at email: martin.kuchar@vsb.cz.